Functional studies on the role of Notch signaling in *Hydractinia* development

James M Gahan[1], Christine E Schnitzler[2,3,4], Timothy Q DuBuc[1], Liam B Doonan[1], Justyna Kanska[1], Sebastian G Gornik[1], Sofia Barreira[4], Kerry Thompson[5], Philipp Schiffer[6], Andreas D Baxevanis[4], Uri Frank[1*]

[1] Centre for Chromosome Biology, School of Natural Sciences, National University of Ireland Galway, Galway, Ireland

[2] Whitney Laboratory for Marine Bioscience, University of Florida, St. Augustine, Florida, USA 320803

[3] Department of Biology, University of Florida, Gainesville, Florida, USA 32611

[4] Division of Intramural Research, National Human Genome Research Institute, National Institutes of Health, Bethesda, MD, USA

[5] Centre for Microscopy and Imaging, Discipline of Anatomy, School of Medicine, National University of Ireland, Galway, Galway, Ireland

[6] Department for Genetics Environment and Evolution, University College London, London, UK

Running title: Notch signaling in *Hydractinia*

Key words: Neurogenesis, Cnidaria, morphogenesis, nematocyte

[*]Corresponding author uri.frank@nuigalway.ie

ABSTRACT

The function of Notch signaling was previously studied in two cnidarians, *Hydra* and *Nematostella*, representing the lineages Hydrozoa and Anthozoa, respectively. Using pharmacological inhibition in *Hydra* and a combination of pharmacological and genetic approaches in *Nematostella*, it was shown in both animals that Notch is required for tentacle morphogenesis and for late stages of stinging cell maturation. Surprisingly, a role for Notch in neural development, which is well documented in bilaterians, was evident in embryonic *Nematostella* but not in adult *Hydra*. Adult neurogenesis in the latter seemed to be unaffected by DAPT, a drug that inhibits Notch signaling. To address this apparent discrepancy we studied the role of Notch in *Hydractinia echinata*, an additional hydrozoan, in all life stages. Using CRISPR-Cas9 mediated mutagenesis, transgenesis, and pharmacological interference we show that Notch is dispensable for *Hydractinia* normal neurogenesis in all life stages but is required for the maturation of stinging cells and for tentacle morphogenesis. Our results are consistent with a conserved role for Notch in morphogenesis and nematogenesis across Cnidaria, and a lineage specific loss of Notch dependence in neurogenesis in hydrozoans.

1. Introduction

Cnidarians (such as corals, sea anemones, hydroids and jellyfish) constitute the sister group to all bilaterian animals (Hejnol et al., 2009; Ryan et al., 2013; Technau and Steele, 2011) and are among the earliest diverging phyla possessing neurons (Galliot and Quiquand, 2011). The cnidarian nervous system consists of three main cell types: sensory neurons, ganglionic neurons, and a phylum-specific sensory/effector cell called a cnidocyte or nematocyte (also known as stinging cells); all of these are thought to develop from a common proliferative precursor population (Miljkovic-Licina et al., 2007; Richards and Rentzsch, 2014). Cnidarian and bilaterian nervous systems are considered homologous, having evolved from their common ancestors some 700 million years ago (Kelava et al., 2015).

Cnidarians employ all major cellular signaling systems known from bilaterians, but the roles many of these pathways play in cnidarian development are not well understood. Notch signaling has been studied in two cnidarians in several contexts but a clear consensus on its function is lacking. Research carried out on the sea anemone *Nematostella*, a member of the cnidarian clade Anthozoa, revealed that embryonic neural progenitors in these animals are epithelial and their numbers are controlled by Notch signaling (Layden and Martindale, 2014; Marlow et al., 2012; Richards and Rentzsch, 2014; Richards and Rentzsch, 2015), similar to their bilaterian counterparts. In hydrozoan cnidarians, however, neurons develop from non-epithelial, migratory stem cells, called i-cells, which are segregated during gastrulation (Gahan et al., 2016; Hager and David, 1997; Leclere et al., 2012; Miljkovic-Licina et al., 2007). Pharmacological inhibition of Notch signaling in adult *Hydra*, a hydrozoan cnidarian, revealed no effect on the numbers of adult neurons (Käsbauer et al., 2007; Khalturin

et al., 2007), but this treatment did affect nematocyte differentiation and tentacle development (Käsbauer et al., 2007; Khalturin et al., 2007; Münder et al., 2013), defects that were also observed in *Nematostella* following pharmacological Notch inhibition (DuBuc et al., 2014; Fritz et al., 2013; Marlow et al., 2012). Hence, the role of Notch in tentacle morphogenesis and nematogenesis seems to be conserved in cnidarians, but its function in neural development requires further research across the phylum. In particular, a role for Notch in de novo adult and embryonic neurogenesis in hydrozoans has yet to be assessed (Rentzsch et al., 2016). Furthermore, genetic approaches have not been utilized in hydrozoan Notch studies.

To extend the knowledge on Notch signaling in cnidarians we focused on *Hydractinia echinata*, a hydrozoan that allows experimental access to all life stages (Flici et al., 2017; Gahan et al., 2016) (Fig. S1). To manipulate Notch signaling, we used genetic gain and loss of function, and pharmacological interference. We analyzed embryos, metamorphosing larvae, and regenerating adults. Our collective data show that Notch signaling is not required for the initial development of at least a subset of neural cells in embryos and adults. However, we confirm the role of Notch signaling in nematocyte differentiation and tentacle morphogenesis.

2. Materials and methods

2.1 Animals

Hydractinia echinata colonies were sampled in Galway Bay, Ireland, and in Roscoff, France. They were cultured in artificial seawater at 18-20ºC under a 10/14 dark/light regime. Animals were fed three times a week with brine shrimp nauplii and twice with ground oyster. Daily spawned gametes from males and females were mixed to

enable fertilization and embryos were allowed to develop to larva stages in plastic Petri dishes. Metamorphosis was induced using a pulse treatment with CsCl (Müller and Buchal, 1973). Metamorphosing animals were positioned on glass coverslips in seawater and allowed to metamorphose.

2.2 Pharmacological inhibition of Notch signaling

N-[N-(3,5-difluorophenacetyl)-l-alanyl]-S-phenylglycine t-butyl ester (DAPT; Abcam, ab120633) was diluted to a stock concentration of 10 mM or 0.1 mM in DMSO and then diluted 1:1000 in artificial seawater to give working solutions of 10 μM and 0.1 μM, respectively. 0.1% DMSO was used as a control in all experiments. Embryos were treated from the 1-2 cell stage until fixation. For metamorphosis experiments animals were first induced with CsCl and then placed in DAPT. Regenerating animals were placed in DAPT immediately post decapitation. In all cases the solution was changed every 24 hours.

2.3 Notch intracellular domain overexpression

In order to generate the Notch intracellular domain (NICD) overexpression construct, the NICD was amplified from cDNA using primers NICDfwd (5'ATGAAAAGGACCTATGGTGCCC3') and NICDrev (5'GCATTGAAATTATATAGTTCGTGCTACAAC3') and cloned into the *β-tubulin*::GFP plasmid using Gibson assembly to generate an NICD-GFP fusion separated by a linker region as used previously (Flici et al., 2017). Injections were carried out as previously described (Millane et al., 2011).

2.4 Staining of nematocysts

Nematocyst staining was carried out as outlined (Szczepanek et al., 2002). Animals were anesthetized, if necessary, for 30 minutes in 4% $MgCl_2$ in 50% ASW/ 50% H_20. Fixation was carried out for 30 minutes at room temperatures in 4% PFA in PBS supplemented with Triton X-100 to a final concentration of 0.3% and EDTA to a final concentration of 10 mM (PBSTE). Following fixation animals were washed three times in PBSTE and then stained overnight in 1:200 DAPI (10 mg/ml) in deionised water. After staining, animals were washed three times in PBSTE and mounted in Fluoromount (Sigma F4680). To combine with antibody staining the immunofluorescence (IF) protocol was carried out as below except EDTA was added to all solutions to a final concentration of 10 mM and DAPI staining was carried out after the secondary antibody.

2.5 mRNA in situ hybridization

Whole mount RNA in-situ hybridizations were carried out as previously published (Gajewski et al., 1996) with minor changes (see supplemental materials and methods).

2.6 Immunofluorescence

Prior to fixation adult stages were anesthetized in 4% $MgCl_2$ in 50% ASW/ 50% H_2O. Animals were fixed in 4% PFA in PBS for 20-60 minutes at room temperature or overnight at 4°C. This was followed by three washes for 10 minutes in PBSTx. For larva an additional wash overnight at 4°C was carried out. Animals were then blocked in 3% BSA in PBSTx for one hour at room temperature before primary antibody (anti acetylated tubulin, Sigma Aldrich T7451; Anti-FRamide (Seipp et al., 2010); Anti-GLWamide (Schmich et al., 1998)) incubation in 3% BSA in PBSTx overnight at 4°C. Animals were then washed four times in PBSTx for at least 10 minutes each. An

additional overnight wash in PBSTx was carried out on larva. Following this, blocking was carried out in 5% goat serum, 3% BSA in PBSTx and then secondary antibody incubation (goat anti-mouse 594, Abcam 150116; goat anti-rabbit 488, Invitrogen A11008) was carried out at room temperature for two hours at a concentration of 1:500 in 5% goat serum, 3% BSA in PBSTx. Animals were then washed once for 20 minutes in 10 ng/µl Hoechst 33258 (25 mg/ml, Sigma B2883) in PBSTx followed by three washes with PBSTx. Animals were mounted in Fluoromount (Sigma F4680).

2.7 Microscopy and cell counting

Fluorescence microscopy was carried out using the Olympus BX51 compound microscope. Confocal microscopy was carried out on either an Olympus FV1000 with an inverted IX71 microscope or Andor revolution spinning disc confocal microscope (Yokagawa CSU_{22}). Image analysis was carried out in all cases using ImageJ (Version 1.6.0_20).

Cell counting was carried out using ImageJ cell counting feature. All counting experiments were carried out in triplicate and at least 8 animals were counted per treatment. For GLWamide$^+$ neurons, confocal z-stacks were counted manually, without projecting. Only the aboral domain of the larva was counted, as this is the site where the majority of the GLWamide$^+$ neurons reside at this stage. For DAPI stained nematocytes images were taken at the surface of the larva. These were then manually counted. Statistical significance was assessed using two-tailed Student t-test if the data were normally distributed (tested by the Shapiro-Wilk test), and the Mann-Whitney U test was carried out otherwise. All data is shown +/- standard deviation

and represent either individual biological replicates or pooled data from 3 replicates as indicated in the figure legends.

CRISPR-Cas9 mutagenesis

Four sgRNAs were generated targeting exons of the *Notch* locus found in both isoforms (Fig. 1C). These sgRNAs were injected into zygotes at a concentration of 125ng/ul each along with 1ug/ul Cas9 protein (PNAbio, CP02) and 1x NEB buffer 3 (NEB). Before injection the mixture was incubated for 10 minutes at 37°C.

Phylogenetic analysis

Phylogenetic analysis was performed using maximum likelihood and Bayesian inference as detailed in the supplemental materials and methods.

3. Results

3.1 Notch signaling components are encoded in the Hydractinia *genome*

We first investigated the presence of Notch pathway components in *Hydractinia*. We found that the *Hydractinia* genome encodes a single *Notch* gene (Fig. 1), several DSL (Delta/Serrate/LAG-2)-type Notch ligands, and a single member of the CSL (CBF1/Suppressor of Hairless/Lag-1) family of transcription factors. *Notch* displayed a dynamic expression pattern throughout the life cycle, as assessed by mRNA in situ hybridization and transcriptomic data (Fig. 1B, D, E). During embryogenesis, *Notch* appeared to be expressed in both the ectoderm and endoderm with higher expression towards the aboral pole, but was somewhat variable between individuals. In the adult polyp, *Notch* was expressed in the body column, excluding the most aboral section, and at the base of the tentacles (Fig 1B). This expression pattern is similar to *HyNotch*

expression in *Hydra* (Münder et al., 2013; Wenger et al., 2016). We also found that *Notch* is alternatively spliced to generate two main isoforms that share all major Notch domains and differ only in the first two exons, which encode EGF repeats (Fig. 1C, F).

3.2 Notch signaling is not required for the normal development of the embryonic RFamide$^+$ and GLWamide$^+$ nervous systems

We then studied the function of Notch signaling, starting with embryonic neurogenesis. For this, we performed CRISPR-Cas9 mediated mutagenesis in *Hydractinia* to target its single *Notch* gene. We developed a strategy whereby we co-inject four sgRNAs with Cas9 protein. To test the efficiency of this approach, genomic DNA was extracted from two independent replicates of pooled, injected larvae. PCR was then carried out, covering the region targeted by all four sgRNAs using primers flanking the four predicted cut sites. Gel electrophoresis revealed extra bands at lower sizes than expected (Fig. S2A). Sanger sequencing has shown either a large deletion resulting from simultaneous cutting by two or more sgRNAs (band 2 in Fig. S2A) or a large resection after cutting with a single sgRNA (band 1 in Fig. S2A). The upper band, i.e. the band at the expected wild type size, was excised, extracted, cloned, and sequenced, revealing the presence of mutations within that region (Fig. S2B). Analysis of multiple clones was used to evaluate the percentage of mutated alleles. Overall, the normal sized alleles were mutated at one or more sites in about 70% of the cases (Fig. S2C) and all scored mutations resulted in frameshifts. Hence, combined with the lower bands, which represented alleles with larger deletions, the rate of mutated alleles was well over 70% in the injected F0 animals using this strategy. We also used a pharmacological approach, by treating developing embryos

with the γ-secretase inhibitor N-[N-(3,5-difluorophenacetyl)-l-alanyl]-S-phenylglycine t-butyl ester (DAPT); this drug prevents release of the Notch intracellular domain (NICD), an essential step in activation of the pathway (Geling et al., 2002; Käsbauer et al., 2007; Micchelli et al., 2003). We then monitored the development of the nervous system in these embryos using markers of early and late neurogenesis. We also stained poly-γ-glutamate$^+$ nematocyst capsules as markers for mature nematocytes (Szczepanek et al., 2002). Overall, genetic or pharmacological inhibition of Notch signaling had no effect on RFamide$^+$ and GLWamide$^+$ neurons but did reduce the numbers of mature nematocytes (Fig. 2), a phenomenon also known from other cnidarians (Käsbauer et al., 2007; Khalturin et al., 2007; Marlow et al., 2012; Richards and Rentzsch, 2015). A detailed analysis of DAPT treated embryos revealed normal numbers and distribution of GLWamide$^+$ and RFamide$^+$ neurons, as well as *Ncol1*$^+$ nematoblasts (i.e. committed, immature nematocytes: Fig. 2A-C) in planula larvae at all concentrations tested, but mature nematocyte numbers were drastically reduced in a dose dependent manner (Fig.2D). Importantly, genetic inhibition of Notch signaling did not compromise the animals' development to metamorphosis competence - a stage that, in *Hydractinia*, requires GLWamide$^+$ neurons (Schmich et al., 1998). Together, these experiments show that Notch signaling is not involved in *Hydractinia* embryonic neurogenesis, at least with respect to RFamide$^+$ and GLWamide$^+$ neurons. We also conclude that Notch signaling plays a role in late nematogenesis, which has also been shown in other cnidarians (Käsbauer et al., 2007; Marlow et al., 2012); in *Hydractinia* this role is limited to later differentiation stages but does not include the control of their early commitment. The absence of a neurogenic effect (i.e. excessive neurons) following Notch inhibition in *Hydractinia* embryos, is markedly different from earlier Notch inhibition experiments

on bilaterian and anthozoan cnidarian embryos that result in an increase in the numbers of neural cells (Chitnis and Kintner, 1996; Hartenstein and Stollewerk, 2015; Henrique et al., 1997; Louvi and Artavanis-Tsakonas, 2006; Richards and Rentzsch, 2015).

3.3 Notch signaling is not involved in development or regeneration of the adult nervous system

We then investigated the effect of Notch signaling inhibition on the formation of the adult nervous system during metamorphosis, a process that transforms a planula larva into a polyp (Fig. S1). Pharmacological inhibition of Notch signaling during the course of metamorphosis resulted in polyps with normal *Rfamide*$^{+}$ oral nervous systems (Fig. 3A). We next studied the effect of inhibition of Notch signaling on adult neurogenesis during regeneration. *Hydractinia* can regenerate a fully functional head, including its nervous system, 2-3 days post-amputation (Bradshaw et al., 2015). Hence, we treated decapitated animals with DAPT, allowed them to regenerate and stained with anti-acetylated tubulin antibodies to mark the nervous system. We found no gross difference in the regenerated, acetylated tubulin positive nervous system between DAPT treated and control animals (Fig. 3B). Finally, we analyzed the effect of DAPT treatment on adult nematogenesis by treating adult polyps with DAPT while feeding them to deplete existing mature nematocytes. This led to a reduction in the number of mature nematocytes (Fig. 3C). Therefore, *Hydractinia* neurogenesis in embryos and adults is similar with regard to Notch function.

3.4 Notch signaling is required for tentacle morphogenesis

Next, we studied the role of Notch signaling in morphogenesis. Notch signaling is frequently used in metazoan development to generate sharp boundaries between domains (Bray, 2006). Indeed, in *Hydra* it was shown to have a role in boundary formation during budding (Münder et al., 2010). DAPT treatment during regeneration led to a block in tentacle formation (Fig. 4A and B), a phenotype also known from other cnidarians (DuBuc et al., 2014; Fritz et al., 2013; Marlow et al., 2012; Münder et al., 2013). However, as shown above, the acetylated tubulin positive oral nervous system in regenerating, Notch inhibited polyps was normal (Fig 3B). Pharmacological or genetic inhibition of Notch signaling during metamorphosis led to a striking reduction in the number of formed tentacles without affecting stolon outgrowth or hypostome development (i.e. the region between the tentacles and the mouth; Fig 4C-E). This is consistent with results obtained in other cnidarians.

Finally, we studied the effect of ectopic *Notch* activation on *Hydractinia* development. For this, we ectopically expressed NICD in *Hydractinia* embryos using random integration transgenesis, which produced transgenic mosaic animals (Fig. S3). These animals developed normally to metamorphosis-competent planula larvae and were then induced to metamorphose. Consistent with the Notch inhibition experiments described above, following metamorphosis induction they developed multiple ectopic tentacles (Fig. 4F), phenotypes never seen in control transgenic animals that expressed a GFP transgene driven by the same promoter (Fig. 4F).

Discussion

Taken together, these results show that Notch signaling in *Hydractinia* is required for tentacle morphogenesis and for late stage nematocyte differentiation, but is

dispensable for the development and normal distribution of Rfamide^{+} and GLWamide^{+} neurons. Given that Notch signaling is generally considered to be a negative regulator of neurogenesis (Hartenstein and Stollewerk, 2015), the lack of a neurogenic effect, i.e. increase in neural cells following Notch inhibition, is striking. Hence, our data not only confirm previous results on adult neurogenesis in *Hydra*, but also extend the understanding of Notch signaling in hydrozoans to adult regeneration, metamorphosis, and embryonic development.

The evolution of Notch signaling as a negative regulator of neurogenesis is debatable, being either a primitive or a derived trait. According to current literature, this function of Notch is present in nearly all studied bilaterians (Hartenstein and Stollewerk, 2015) and in anthozoan cnidarians (Layden and Martindale, 2014; Marlow et al., 2012; Richards and Rentzsch, 2015). Our data, and those of previous authors working on *Hydra* (Käsbauer et al., 2007; Khalturin et al., 2007), suggest that it is absent in hydrozoans. Given the phylogenetic position of the Anthozoa as a basal cnidarian clade (Bridge et al., 1992; Zapata et al., 2015), with Hydrozoa considered derived, a scenario of a primitive Notch function in neurogenesis inhibition in eumetazoans is parsimonious (Fig. 5). Hence, the absence of this trait in *Hydra* and *Hydractinia* reflects a specific loss in the hydrozoan lineage rather than multiple acquisitions in other lineages. Of note, early neurogenesis in the annelid *Platynereis* is Notch independent (Gazave et al., 2017), like in hydrozoans, and could represent an additional, independent loss. Analysis of the role of Notch signaling in other cnidarian clades and in the basal bilaterian phylum, Xenacoelomorpha, would help resolve this issue.

Other than most studied animals, anthozoan cnidarians included, whose neuronal progenitors are epithelial (Hartenstein and Stollewerk, 2015; Richards and Rentzsch, 2014), hydrozoan neural cells develop from migratory, non-epithelial stem cells, called i-cells that also give rise to non-neural cell types (Gahan et al., 2016). Furthermore, neurogenesis occurs in both the ectoderm and endoderm in *Nematostella*. Hydrozoan i-cells are first found in the endoderm, and embryonic neurogenesis occurs within this tissue (Flici et al., 2017; Martin, 1990), also pointing to a derived mode of neurogenesis in hydrozoans. Co-occurrence of the i-cell lineage, exclusively endodermal embryonic neurogenesis, and the loss of Notch mediated neurogenesis inhibition in hydrozoans are consistent with a link between these phenomena.

Author contributions

JMG and UF conceived the study; JMG performed the experiments; CES, and ADB provided genomics data; TQD performed *Notch* in situ hybridization; LBD, SGG, and SB performed transcriptome analysis; JK provided gene expression data, PS provided transcriptomic data on *Notch* isoforms; KT performed spinning disk confocal microscopy; JMG and UF wrote the paper.

Acknowledgements

We thank members of our lab for comments and discussions. We are indebted to Werner A Müller for drawings in Fig. 3. Thanks are also due to the staff of the Station Biologique Roscoff, France for providing *Hydractinia echinata* colonies. We also thank Thomas Leitz for providing GLWamide antibodies. This research was funded by Science Foundation Ireland (SFI) through a Principal Investigator Award to UF (grant No. 11/PI/1020). It was also supported in part by the Intramural Research

Program of the National Human Genome Research Institute, National Institutes of Health (NIH). JMG was a recipient of a Beckman Fund Scholarship. KT was funded by the Irish Higher Education Authority, Programme for Research in Third Level Institutions. SGG was funded by a Starting Investigator Research Grant (SIRG) from SFI and by a Marie Curie Incoming International Fellow award. TQD was funded by an EMBO Long Term Fellowship.

REFERENCES

Bradshaw, B., Thompson, K., Frank, U., 2015. Distinct mechanisms underlie oral vs aboral regeneration in the cnidarian *Hydractinia echinata*. eLife 4.

Bray, S.J., 2006. Notch signalling: a simple pathway becomes complex. Nat Rev Mol Cell Biol 7, 678-689.

Bridge, D., Cunningham, C.W., Schierwater, B., DeSalle, R., Buss, L.W., 1992. Class-level relationships in the phylum Cnidaria: Evidence from mitochondrial genome structure. PNAS 89, 8750-8753.

Chitnis, A., Kintner, C., 1996. Sensitivity of proneural genes to lateral inhibition affects the pattern of primary neurons in Xenopus embryos. Development 122, 2295-2301.

DuBuc, T.Q., Traylor-Knowles, N., Martindale, M.Q., 2014. Initiating a regenerative response; cellular and molecular features of wound healing in the cnidarian Nematostella vectensis. BMC biology 12, 24.

Flici, H., Schnitker, N., Millane, R.C., Govinden, G., Houlihan, A., Boomkamp, S.D., Shen, S., Baxevanis, A.D., Frank, U., 2017. An evolutionarily conserved SoxB-Hdac2 crosstalk regulates neurogenesis in a cnidarian. Cell reports 18, 1395-1409.

Fritz, A.E., Ikmi, A., Seidel, C., Paulson, A., Gibson, M.C., 2013. Mechanisms of tentacle morphogenesis in the sea anemone *Nematostella vectensis*. Development 140, 2212-2223.

Gahan, J.M., Bradshaw, B., Flici, H., Frank, U., 2016. The interstitial stem cells in Hydractinia and their role in regeneration. Curr Opin Genet Dev 40, 65-73.

Gajewski, M., Leitz, T., Schloherr, J.R., Plickert, G.N., 1996. LWamides from Cnidaria constitute a novel family of neuropeptides with morphogenetic activity. Roux's Arch Dev Biol. 205.

Galliot, B., Quiquand, M., 2011. A two-step process in the emergence of neurogenesis. Eur J Neurosci 34, 847-862.

Gazave, E., Lemaitre, Q.I., Balavoine, G., 2017. The Notch pathway in the annelid Platynereis: insights into chaetogenesis and neurogenesis processes. Open Biol 7.

Geling, A., Steiner, H., Willem, M., Bally-Cuif, L., Haass, C., 2002. A γ-secretase inhibitor blocks Notch signaling in vivo and causes a severe neurogenic phenotype in zebrafish. EMBO Rep 3, 688-694.

Hager, G., David, C.N., 1997. Pattern of differentiated nerve cells in hydra is determined by precursor migration. Development 124, 569-576.

Hartenstein, V., Stollewerk, A., 2015. The Evolution of Early Neurogenesis. Dev Cell 32, 390-407.

Hejnol, A., Obst, M., Stamatakis, A., Ott, M., Rouse, G.W., Edgecombe, G.D., Martinez, P., Baguna, J., Bailly, X., Jondelius, U., Wiens, M., Muller, W.E., Seaver, E., Wheeler, W.C., Martindale, M.Q., Giribet, G., Dunn, C.W., 2009. Assessing the root of bilaterian animals with scalable phylogenomic methods. Proc Biol Sci 276, 4261-4270.

Henrique, D., Hirsinger, E., Adam, J., Le Roux, I., Pourquie, O., Ish-Horowicz, D., Lewis, J., 1997. Maintenance of neuroepithelial progenitor cells by Delta-Notch signalling in the embryonic chick retina. Curr Biol 7, 661-670.

Käsbauer, T., Towb, P., Alexandrova, O., David, C.N., Dall'Armi, E., Staudigl, A., Stiening, B., Böttger, A., 2007. The Notch signaling pathway in the cnidarian Hydra. Developmental Biology 303, 376-390.

Kelava, I., Rentzsch, F., Technau, U., 2015. Evolution of eumetazoan nervous systems: insights from cnidarians. Philos Trans R Soc Lond B Biol Sci 370.
Khalturin, K., Anton-Erxleben, F., Milde, S., Plotz, C., Wittlieb, J., Hemmrich, G., Bosch, T.C.G., 2007. Transgenic stem cells in Hydra reveal an early evolutionary origin for key elements controlling self-renewal and differentiation. Dev Biol 309, 32-44.
Layden, M.J., Martindale, M.Q., 2014. Non-canonical Notch signaling represents an ancestral mechanism to regulate neural differentiation. Evodevo 5, 30.
Leclere, L., Jager, M., Barreau, C., Chang, P., Le Guyader, H., Manuel, M., Houliston, E., 2012. Maternally localized germ plasm mRNAs and germ cell/stem cell formation in the cnidarian Clytia. Dev Biol 364, 236-248.
Louvi, A., Artavanis-Tsakonas, S., 2006. Notch signalling in vertebrate neural development. Nat Rev Neurosci 7, 93-102.
Marlow, H., Roettinger, E., Boekhout, M., Martindale, M.Q., 2012. Functional roles of Notch signaling in the cnidarian Nematostella vectensis. Developmental Biology 362, 295-308.
Martin, V.J., 1990. Development of Nerve Cells in Hydrozoan Planulae: III. Some Interstitial Cells Traverse the Ganglionic Pathway in the Endoderm. Biol Bull 178, 10-20.
Micchelli, C.A., Esler, W.P., Kimberly, W.T., Jack, C., Berezovska, O., Kornilova, A., Hyman, B.T., Perrimon, N., Wolfe, M.S., 2003. Gamma-secretase/presenilin inhibitors for Alzheimer's disease phenocopy Notch mutations in Drosophila. Faseb j 17, 79-81.
Miljkovic-Licina, M., Chera, S., Ghila, L., Galliot, B., 2007. Head regeneration in wild-type hydra requires de novo neurogenesis. Development 134, 1191-1201.
Millane, R.C., Kanska, J., Duffy, D.J., Seoighe, C., Cunningham, S., Plickert, G., Frank, U., 2011. Induced stem cell neoplasia in a cnidarian by ectopic expression of a POU domain transcription factor. Development 138, 2429-2439.
Müller, W.A., Buchal, G., 1973. Metamorphoseinduktion bei Planulalarven. II. Induktion durch monovalente Kationen: Die Bedeutung des Gibbs-Donnan Verhältnisses und der Ka+Na+-ATPase. Wilhelm Roux Arch. 173, 122-135.
Münder, S., Käsbauer, T., Prexl, A., Aufschnaiter, R., Zhang, X., Towb, P., Böttger, A., 2010. Notch signalling defines critical boundary during budding in Hydra. Developmental Biology 344, 331-345.
Münder, S., Tischer, S., Grundhuber, M., Buchels, N., Bruckmeier, N., Eckert, S., Seefeldt, C.A., Prexl, A., Kasbauer, T., Bottger, A., 2013. Notch-signalling is required for head regeneration and tentacle patterning in Hydra. Dev Biol 383, 146-157.
Rentzsch, F., Layden, M., Manuel, M., 2016. The cellular and molecular basis of cnidarian neurogenesis. Wiley Interdisciplinary Reviews: Developmental Biology.
Richards, G.S., Rentzsch, F., 2014. Transgenic analysis of a SoxB gene reveals neural progenitor cells in the cnidarian Nematostella vectensis. Development.
Richards, G.S., Rentzsch, F., 2015. Regulation of Nematostella neural progenitors by SoxB, Notch and bHLH genes. Development 142, 3332-3342.
Ryan, J.F., Pang, K., Schnitzler, C.E., Nguyen, A.D., Moreland, R.T., Simmons, D.K., Koch, B.J., Francis, W.R., Havlak, P., Smith, S.A., Putnam, N.H., Haddock,

S.H.D., Dunn, C.W., Wolfsberg, T.G., Mullikin, J.C., Martindale, M.Q., Baxevanis, A.D., 2013. The Genome of the Ctenophore Mnemiopsis leidyi and Its Implications for Cell Type Evolution. Science 342, 1242592-1242592.

Schmich, J., Trepel, S., Leitz, T., 1998. The role of GLWamides in metamorphosis of *Hydractinia echinata*. Dev Genes Evol 208, 267-273.

Seipp, S., Schmich, J., Will, B., Schetter, E., Plickert, G., Leitz, T., 2010. Neuronal cell death during metamorphosis of Hydractina echinata (Cnidaria, Hydrozoa). Invert Neurosci 23, 23.

Szczepanek, S., Cikala, M., David, C.N., 2002. Poly-{gamma}-glutamate synthesis during formation of nematocyst capsules in Hydra. J Cell Sci 115, 745-751.

Technau, U., Steele, R.E., 2011. Evolutionary crossroads in developmental biology: Cnidaria. Development 138, 1447-1458.

Wenger, Y., Buzgariu, W., Galliot, B., 2016. Loss of neurogenesis in Hydra leads to compensatory regulation of neurogenic and neurotransmission genes in epithelial cells. Philos Trans R Soc Lond B Biol Sci 371.

Zapata, F., Goetz, F.E., Smith, S.A., Howison, M., Siebert, S., Church, S.H., Sanders, S.M., Ames, C.L., McFadden, C.S., France, S.C., Daly, M., Collins, A.G., Haddock, S.H.D., Dunn, C.W., Cartwright, P., 2015. Phylogenomic Analyses Support Traditional Relationships within Cnidaria. Plos One 10, e0139068.

FIGURE LEGENDS

Figure 1. *Notch* phylogeny, expression, genomic architecture and alternative splicing. (A) Unrooted maximum likelihood/Baysian phylogeny of *Hydractinia echinata Notch*; scale bar = nucleotide changes per site. (B) In-situ hybridization showing *Notch* mRNA expression patterns at 12, 24 and 96 hours post fertilization (hpf), and adult polyp; scale bar = 100 μm in embryos and larva, and 300 μm in the polyp. (C) *Notch* genomic locus showing CRISPR-Cas9 guide RNA sites, alternative exons and the complete architecture of the mRNA for the two notch isoforms. (D) *Notch* expression levels in *Hydractinia* eggs (maternal transcripts), larvae, feeding, and male and female polyps. (E) Ratio of expression of *Notch* isoforms in percent across the same life stages shown in (D). (F) Domain structure of Notch isoform 1 and isoform 2 alongside *Drosophila* Notch and Human Notch1.

Figure 2. Notch signaling is not involved in embryonic neural commitment. (**A**) Pharmacological inhibition of γ-secretase by DAPT during embryogenesis does not affect the pattern and numbers of GLWamide$^+$ neurons in larvae. (**B,C**) DAPT treatment during embryogenesis does not affect the pattern of RFamide$^+$ neurons (B) or the expression pattern of *Ncol1* (C) in larvae. (**D**) γ-secretase inhibition leads to a dose dependent loss of mature poly-γ-glutamate positive nematocysts in larvae. (**E, F**) CRISPR-Cas9 mediated mutagenesis of *Notch* does not affect the number of GLWamide$^+$ neurons (E) but causes a reduction in the numbers of poly-γ-glutamate$^+$ nematocysts (F). Scale bars: 10 μm in (A, B and D) and 40 μm in (C). Data represents combined counting from 3 independent biological replicates. * Student t-test with $p<0.05$. ** Student t-test with $p<0.0001$. *** Mann-Whitney U-test with $p<0.05$.

Figure 3. Notch signaling is does not play a role in adult neural commitment. (**A**) Pharmacological inhibition of γ-secretase by DAPT during metamorphosis does not affect the pattern of RFamide$^+$ neurons in the oral nerve net. (**B**) γ-secretase inhibition following decapitation does not affect the regeneration of the oral nervous system (**C**) DAPT treatment over 5 days with daily feeding causes a reduction in the numbers of poly-γ-glutamate$^+$ nematocysts. Asterisk marks the oral pole in all images. Scale bars: 50 μm in (A), 10 μm in (B), 250 μm in (C).

Figure 4. Notch signaling is required for tentacle formation. (**A, B**) DAPT treatment following decapitation inhibits tentacle but not hypostome regeneration. (**C, D**) DAPT treatment during metamorphosis blocks tentacle development but has no effect on hypostome, body column or stolon formation. (**E**) CRISPR-Cas9 mediated mutagenesis results in defective tentacle patterning during metamorphosis. (**F**) Ectopic expression of NICD leads to the development of ectopic tentacles. Scale bars: 250 μm in (A), 40 μm in (C) 100 μm in (E) and (F). Asterisk marks the oral pole in all images. * Student t-test with $p<0.0001$. ** Student t-test with $p<0.000001$.

Figure 5. A hypothetical scenario for the evolution of neurogenesis in hydrozoans. Ancestral neural progenitors were segregated from epithelial cells via Notch mediated lateral inhibition. In the hydrozoans ancestor, neural progenitors became Notch independent through a yet unknown, mechanism.

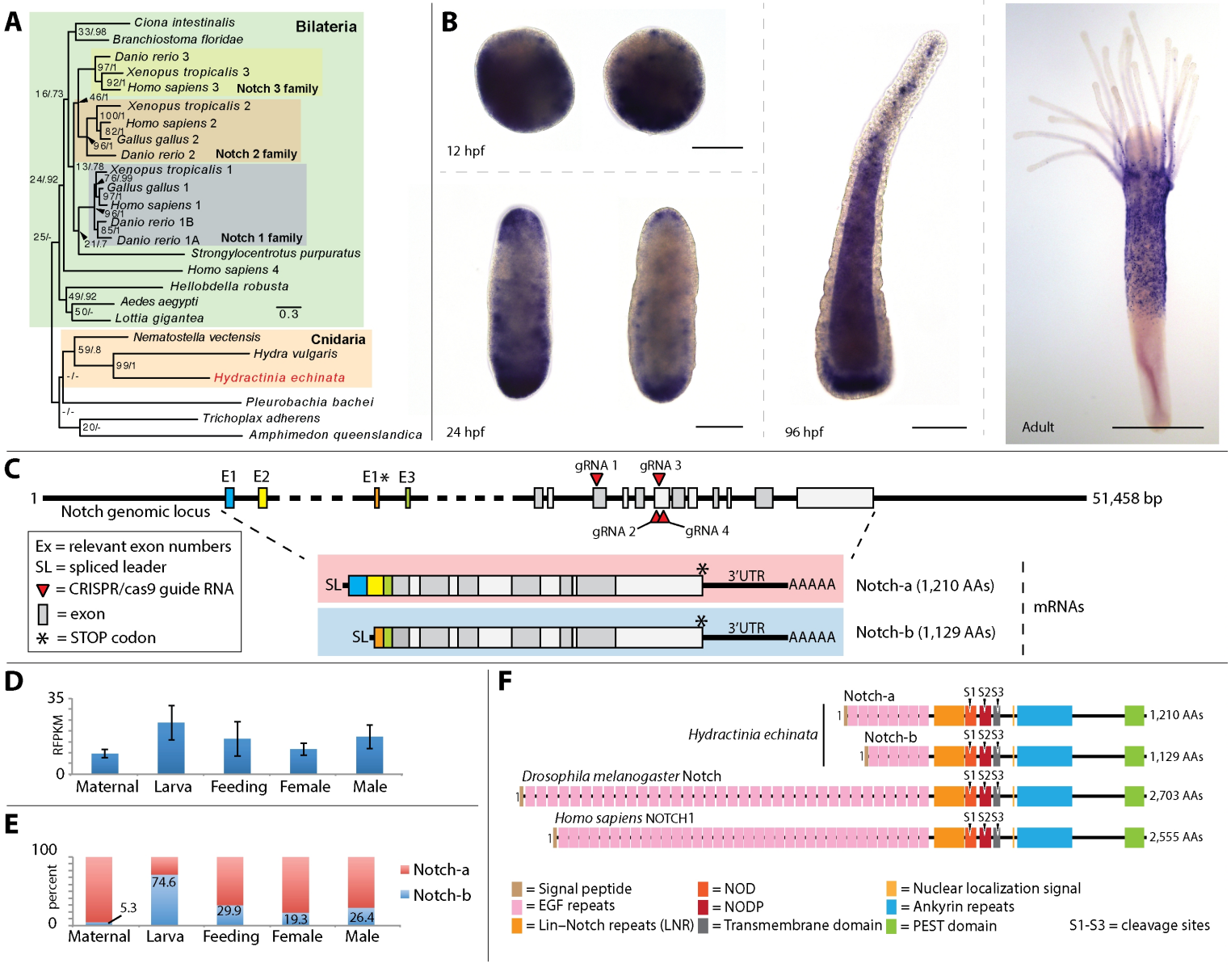
A
Bilateria
Ciona intestinalis
Branchiostoma floridae
Notch 3 family
Danio rerio 3
Xenopus tropicalis 3
Homo sapiens 3
Notch 2 family
Xenopus tropicalis 2
Homo sapiens 2
Gallus gallus 2
Danio rerio 2
Notch 1 family
Xenopus tropicalis 1
Gallus gallus 1
Homo sapiens 1
Danio rerio 1B
Danio rerio 1A
Strongylocentrotus purpuratus
Homo sapiens 4
Hellobdella robusta
Aedes aegypti
Lottia gigantea
0.3
Cnidaria
Nematostella vectensis
Hydra vulgaris
Hydractinia echinata
Pleurobachia bachei
Trichoplax adherens
Amphimedon queenslandica
B
12 hpf
24 hpf
96 hpf
Adult
C
Notch genomic locus
1
51,458 bp
E1
E2
E1*
E3
gRNA 1
gRNA 3
gRNA 2
gRNA 4
Ex = relevant exon numbers
SL = spliced leader
= CRISPR/cas9 guide RNA
= exon
= STOP codon
SL
3'UTR
AAAAA
Notch-a (1,210 AAs)
Notch-b (1,129 AAs)
mRNAs
D
RFPKM
35
0
Maternal
Larva
Feeding
Female
Male
E
percent
100
0
5.3
74.6
29.9
19.3
26.4
Notch-a
Notch-b
F
Hydractinia echinata
Notch-a
Notch-b
1,210 AAs
1,129 AAs
Drosophila melanogaster Notch
2,703 AAs
Homo sapiens NOTCH1
2,555 AAs
S1 S2 S3
= Signal peptide
= EGF repeats
= Lin–Notch repeats (LNR)
= NOD
= NODP
= Transmembrane domain
= Nuclear localization signal
= Ankyrin repeats
= PEST domain
S1-S3 = cleavage sites

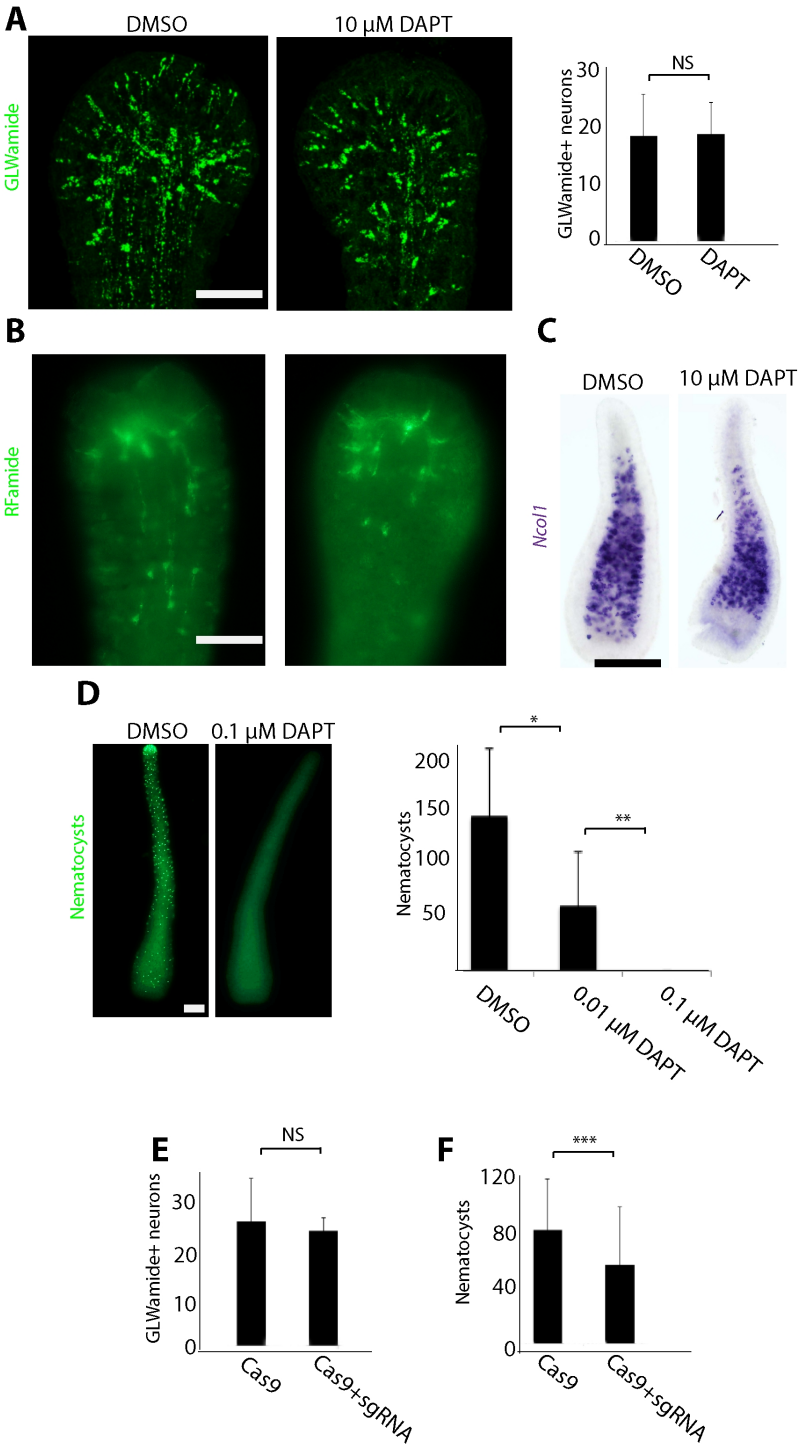
A
DMSO
10 µM DAPT
GLWamide
GLWamide+ neurons
NS
30
20
10
0
DMSO
DAPT
B
RFamide
C
DMSO
10 µM DAPT
Ncol1
D
DMSO
0.1 µM DAPT
Nematocysts
*
**
200
150
100
50
DMSO
0.01 µM DAPT
0.1 µM DAPT
E
NS
GLWamide+ neurons
30
20
10
0
Cas9
Cas9+sgRNA
F
***
Nematocysts
120
80
40
0
Cas9
Cas9+sgRNA

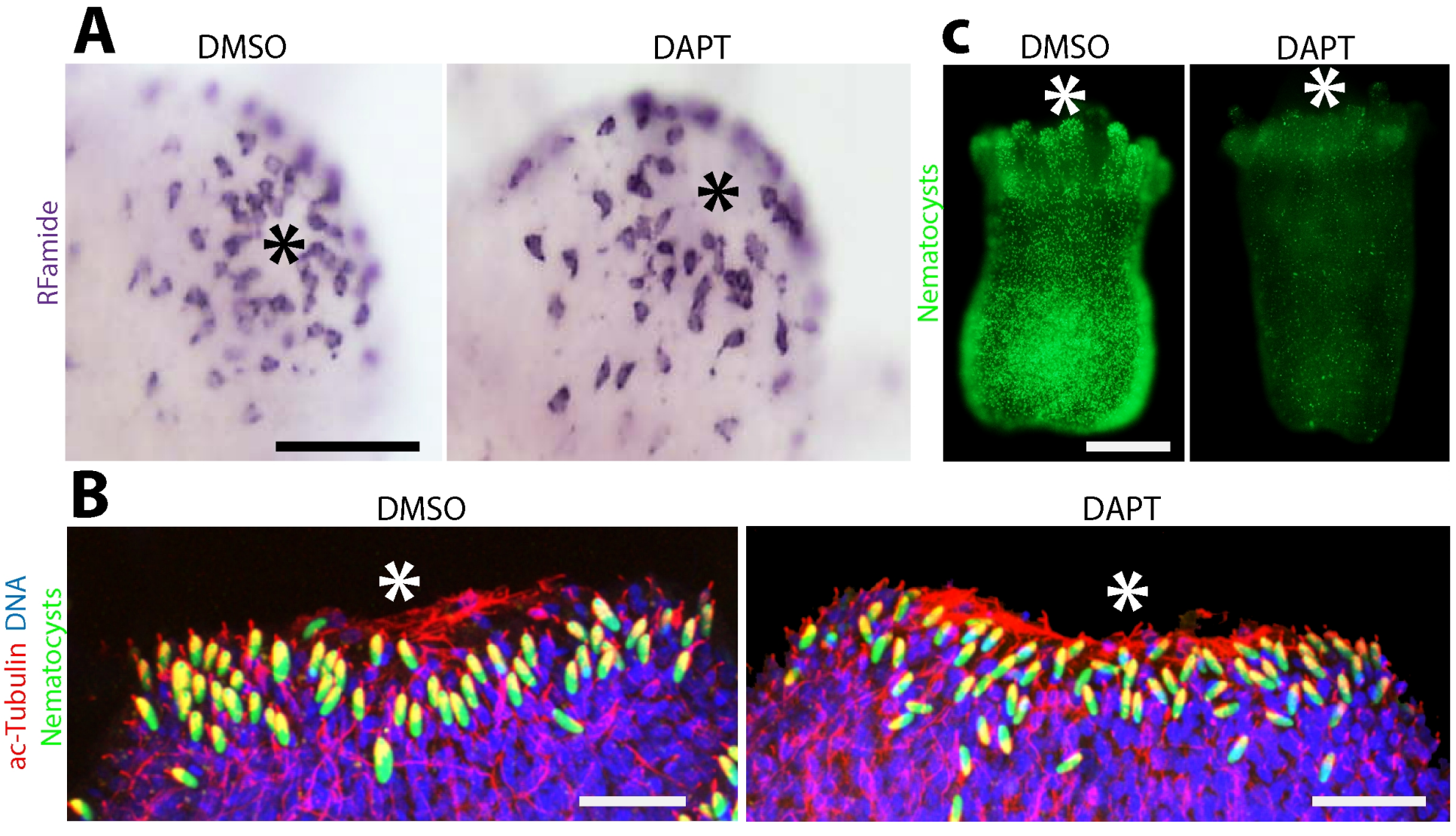
A
DMSO
DAPT
RFamide
C
DMSO
DAPT
Nematocysts
B
DMSO
DAPT
ac-Tubulin DNA
Nematocysts

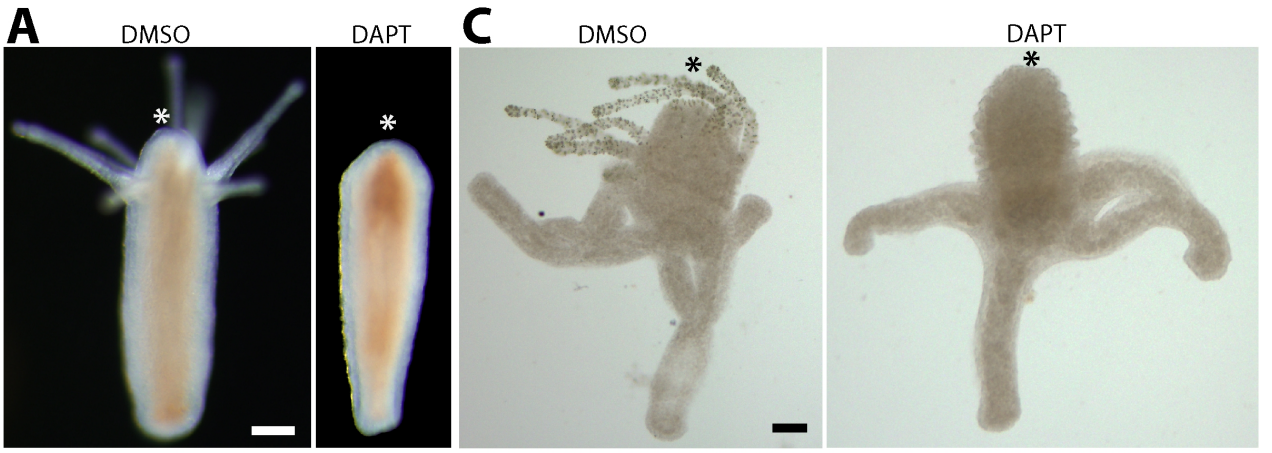

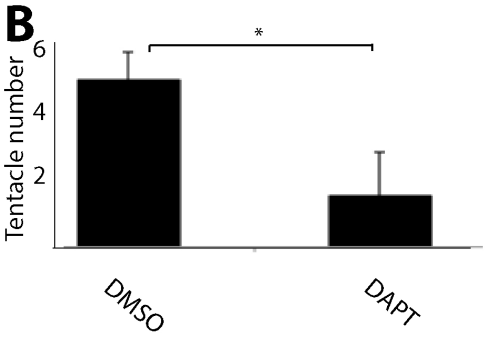

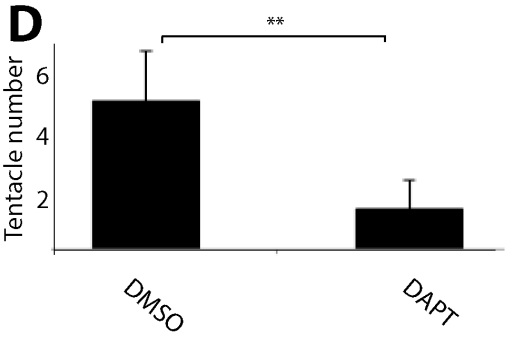

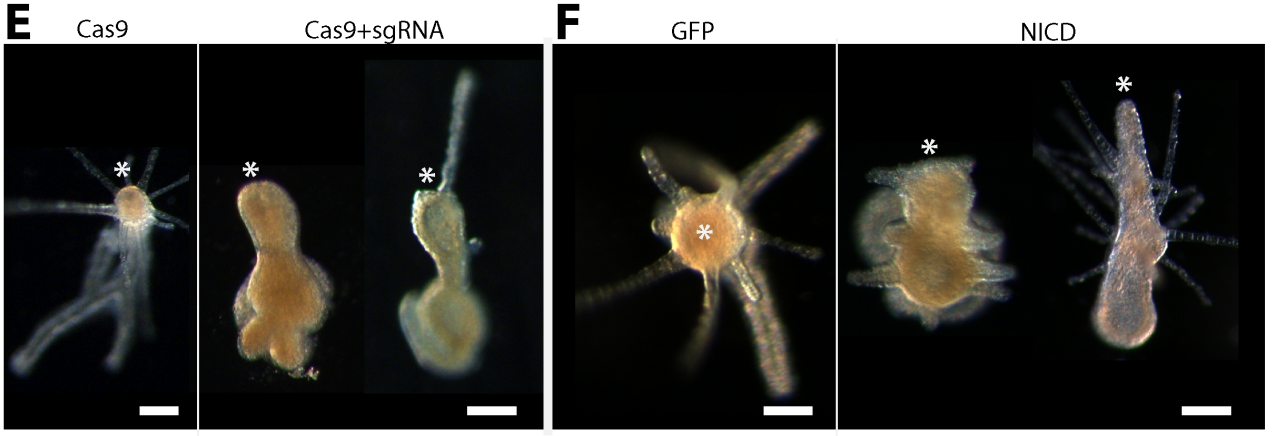

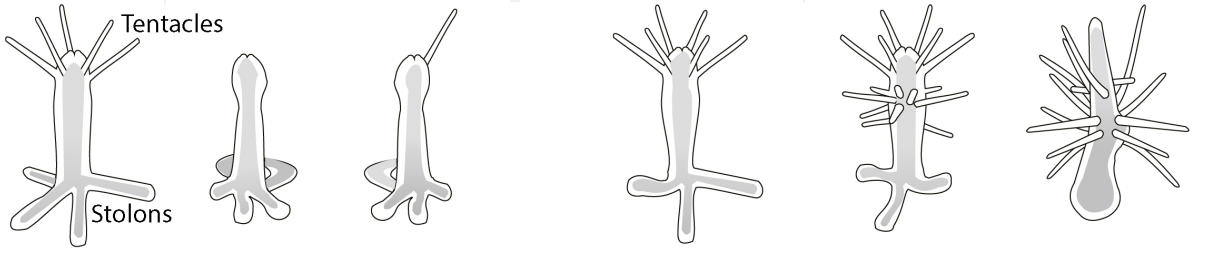

Treatment	Normal tentacles	Abnormal tentacles
Cas9 only	25/26	1/26
Cas9 + sgRNA	13/30	17/30

Treatment	Normal tentacles	Ectopic tentacles
GFP control	37/37	0/37
NICD	30/40	10/40

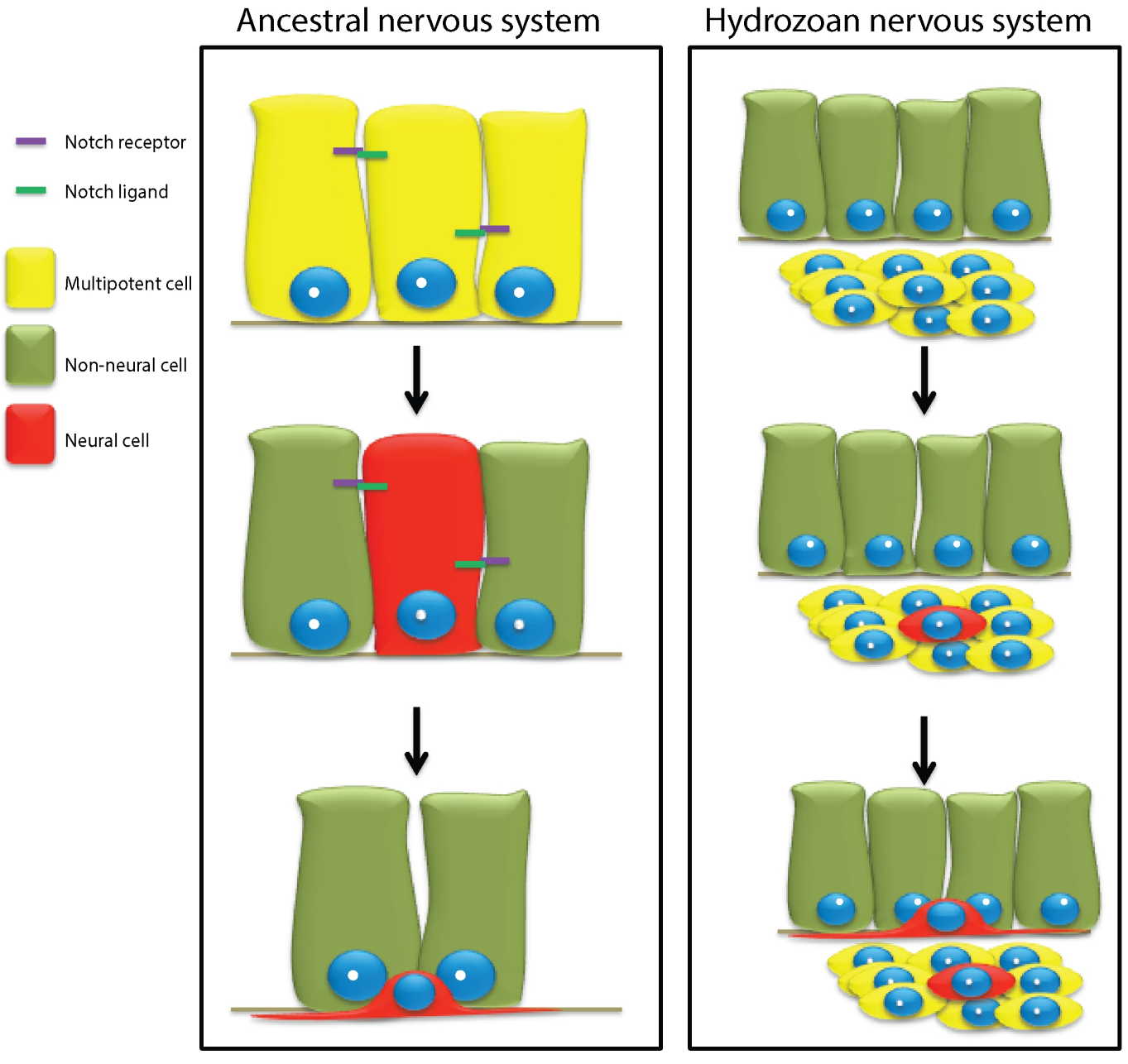
Ancestral nervous system
Hydrozoan nervous system
Notch receptor
Notch ligand
Multipotent cell
Non-neural cell
Neural cell

SUPPLEMENTAL MATERIALS AND METHODS

Notch phylogeny

Hydractinia notch protein sequence, as well as those for Notch ligands and CBF proteins, were obtained from a transcriptome generated as described (Török et al., 2016). All sequences have been submitted to GenBank with accession numbers as follows: Notch-a (KY882021), Notch-b (KY882022), Delta1 (KY882018), Delta2 (KY882019), Jagged1 (KY882020), Su(H) (KY882023).The notch protein sequences of other metazoans were retrieved from published alignments (Gazave et al., 2009). *Hydractinia echinata* Notch (this study), *Hydra vulgaris* notch (GenBank Accession ABV68547.1) and *Pleurobrachia bachei* notch (http://neurobase.rc.ufl.edu/pleurobrachia/browse) sequences were added to the existing alignments (Gazave et al., 2009) using MAFFT (v1.3.3) in Geneious (version R8; Biomatters). EGF repeat domains were excluded from the alignments due to their variability across species (see (Gazave et al., 2009) for details). Thus, notch alignments start only at the notch LNR domain and continue to the end of the protein. As a consequence, both *Hydractinia* Notch isoforms differ only in the EGF domain repeat number converge (Fig. 1). Bootstrapped maximum likelihood phylogenies were prepared with RAxML (version 7.2.8) using a WAG substitution matrix and executing 500 rapid bootstrap inferences and thereafter a thorough ML search. All free model parameters were estimated by RAxML using a gamma model of rate heterogeneity up to an accuracy of 0.1 Log Likelihood units. Bayesian analysis was performed using MrBayes 3.2.6 in Geneious using the WAG fixed model and gamma rate variation. Markov Chain Monte Carlo runs of 1,100,000 generations were calculated with trees sampled every 200 generations and with a prior burn-in of 110,000 generations. The best-scoring tree was visualized using FigTree (v1.4.2; http://tree.bio.ed.ac.uk/software/figtree) and annotated in Adobe Illustrator CS6.

Notch isoforms identification and expression analysis

RNA was extracted from adult male and female sexual polyps, adult feeding polyps, and developmental stages as described (Török et al., 2016). Any contaminating material not representing the selected stage was removed from the samples before processing and seawater replaced by three washes in sterile 0.5 M NaCl. Total RNA was isolated by guanidinium thiocyanate and CsCl cushion ultracentrifugation (Chirgwin et al., 1979). cDNA synthesis for Illumina HiSeq sequencing was conducted at the Cologne Center for Genomics (Cologne, Germany). 100-bp paired-end reads with 170 bp insert size were sequenced. We used FastQC (http://www.bioinformatics.babraham.ac.uk/projects/fastqc/ [last accessed 23/10/2016]) to

validate data quality and Trimmomatic (Bolger et al., 2014) to clean adapters and weakly supported bases. We assembled each single transcriptome, as well as all data combined with the Trinity pipeline (Haas et al., 2013) and calculated FPKM values with RSEM (Li and Dewey, 2011) and edgeR (Robinson et al., 2010) as integrated in this pipeline. We then used the clc mapper v.5.0 (CLC Bio, Qiagen) to map RNA-Seq data to genomic contigs containing the predicted notch gene to analyze transcript coverage. *Notch* isoforms were identified by mapping RNA reads from above (clc mapper results) for various life stages of *Hydractinia* to the genomic *Notch* locus using tophat2 (invoking bowtie2) (Kim et al., 2013). We then used cufflinks (version 2.2.1) (Trapnell et al., 2012) and stringtie (version 1.3.0) (Pertea et al., 2015) to assemble isoform transcripts. Overall expression analysis using Trinity (see above) was not sensitive enough to pick up both Notch isoforms, thus, the relative expression between isoforms was determined as follows: the number of reads mapped to the first shared exon (E3; Fig. 1C) of the two isoforms was counted. Following this, the number of reads mapped to exon 1 of each isoform (E1, E1*; Fig. 1C) were also counted and normalized to the read number of the first shared exon (E3) and results expressed in percentage of total reads mapped to E1 and E1*.

Whole mount RNA is-situ hybridisations

Polyps were anaesthetized for 30 minutes in 4% $MgCl_2$ in 50% ASW/ 50% H_2O. Animals were then fixed in 4% PFA in HEPES buffer (100 mM HEPES, 4 mM $MgSO_4$, 140 mM NaCl) for one hour at room temperature or overnight at 4°C. Animals were then washed three times for five minutes in 0.1% TWEEN20 in PBS (PBST). Animals were then dehydrated through a series of 25%, 50%, 75% and 100% methanol with each step incubated for ten minutes. Animals were then stored at -20°C for later use or used immediately. Animals were rehydrated through a reverse series of methanol, as above, followed by three washes in PBST for five minutes each. This was followed by incubation for 15 minutes at 95°C in PBST. Animals were then washed once with 1x triethylamine (TEA), 0.06% acetic acid in 1X TEA, 0.12% acetic acid in 1X TEA and PBST for five minutes each. Animals were then fixed for 20 minutes in 4% PFA in PBS followed by three washes in 0.3% Triton X-100 in PBS (PBSTx) for five minutes each. Blocking was then carried in 2 mg/ml yeast tRNA for ten minutes. An equal volume of hybridization buffer (50% deionised formamide, 0.1 mg/ml yeast tRNA, 0.1 mg/ml Heparin, 5x SCC, 0.1% Tween 20) was then added and incubated for a further ten minutes. Pre-hybridization was then carried out overnight at 50°C in hybridization buffer. Probes were diluted to a concentration of 40 ng/ml in hybridization

buffer and hybridization was carried out overnight at 50°C. Following hybridization animals were washed once in hybridization buffer at 50°C for five minutes followed by one hour in wash one (50% formamide, 2x SCC, 0.1% TWEEN 20) at 50°C, 15 minutes in wash two (2x SCC, 0.1% TWEEN 20) at 50°C, 15 minutes in wash three (0.2x SCC, 0.1% TWEEN 20) at 50°C and 15 minutes in wash three at room temperature. This was followed by three washes for five minutes in PBSTx and then one hour blocking in 3% bovine serum albumin (BSA) in PBSTx. Animals were incubated in 1:2000 antibody (Anti-DIG AP, Roche) in 3% BSA/PBSTx overnight at 4°C followed by thee washes with PBSTx. Three washes in alkaline phosphatase (AP) buffer (100 mM NaCl, 100 mM Tris-HCl pH 9.5, 50 mM $MgCL_2$, 0.1% Tween 20) were then performed prior to staining. Animals were stained in NBT/BCIP solution (225 ug/ml NBT, 175 ug/ml BCIP in AP buffer) and staining was monitored under a microscope. Once staining was completed animals were washed three times in 10 mM EDTA in PBSTx and mounted in 90% glycerol.

Notch in-situ hybridization required a more stringent protocol where tissue was pre-fixed in 4% PFA in filtered artificial seawater containing 0.2% glutaraldehyde for ninety seconds. Then, tissue was fixed for one hour at 4˚C in 4% PFA in filtered artificial seawater. Samples were then washed five times for five minutes in PBST, followed by dehydration in a series of 25%, 50%, 75% and 100% methanol. Additionally, samples were washed in 75% methanol / 25% acetone, then 80% acetone / 20% methanol to help with permeabilization. Samples were stored in 100% methanol at -20°C. Tissue hybridization was carried out overnight at 55°C, and Notch probes were diluted to a concentration of 1 ng/ml. Subsequent washes and development after hybridization were the same as protocols developed for *Nematostella vectensis* (Wolenski et al., 2013).

Ncol1 and *Rfamide* probes were as previously published (Kanska and Frank, 2013). *Notch* probes were generated using the same protocol. Briefly primers containing Sp6 and T7 sites (FwdT7:5'GATCATAATACGACTCACTATAGGGCTGGTGGTTGTTTCTCTACAACT3', RevSP6:5'TAGCAATTTAGGTGACACTATAGAAGATGCAATGCGGTATAACCCT3') were used to amplify a ~800bp fragment of the *Notch* gene from cDNA and this was then used as template for probe synthesis as previously described.

SUPPLEMENTAL FIGURES

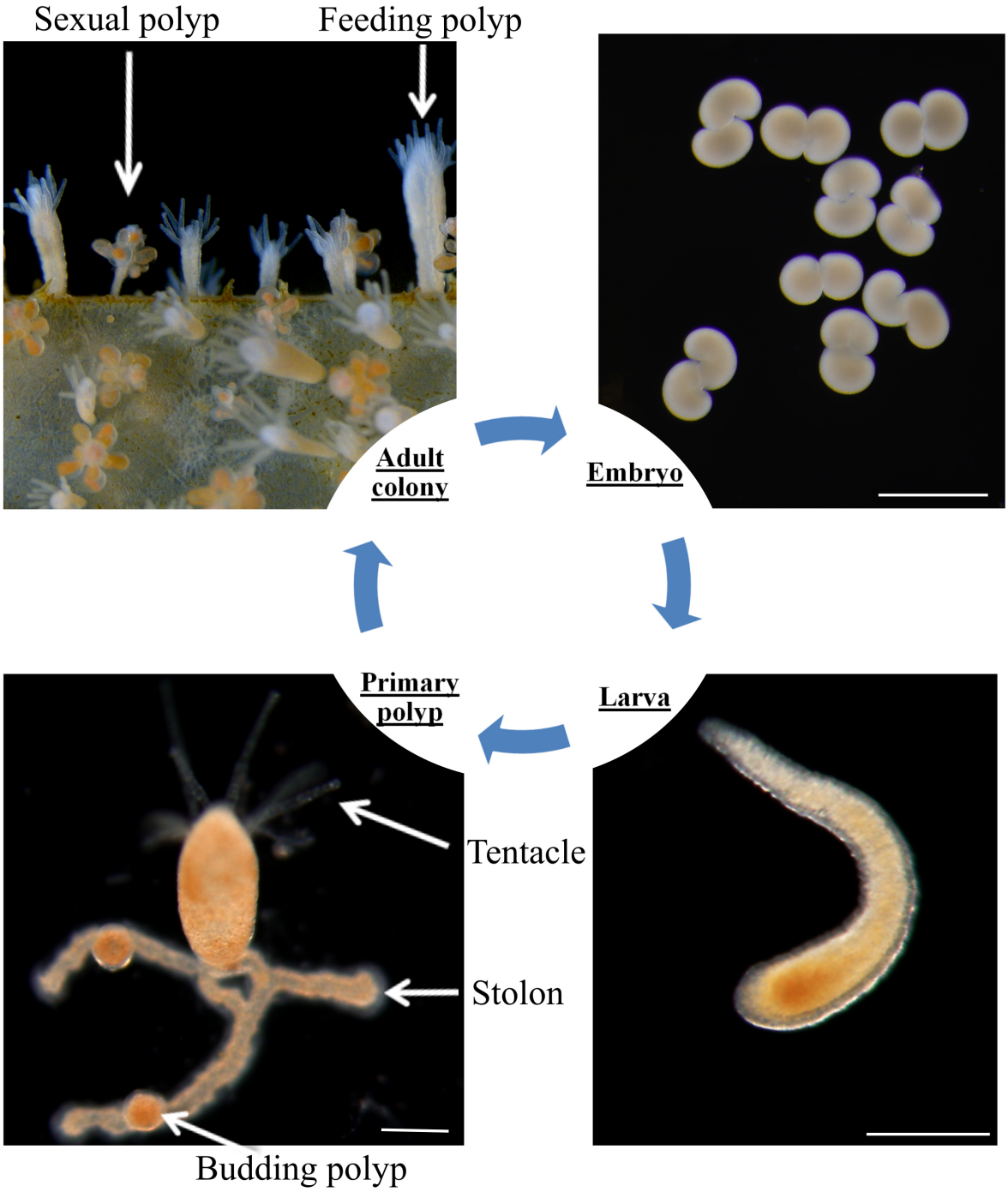

Figure S1. The *Hydractinia* life cycle. Mature colonies spawn daily in a light induced cycle and fertilization occurs in the water column. Embryonic development gives rise to a motile planula larva within 2-3 days. The larva can be induced to undergo metamorphosis and give rise to a sessile primary polyp consisting of a cylindrical body column with an oral 'head' that includes a mouth and hypostome surrounded by a ring of tentacles. The polyp is attached to the substratum at the aboral side and a gastrovascular network of tubes - known as stolon - connects all polyps in a colony. The stolons grow outwards from the primary polyp and bud new polyps at regular intervals. The stolonal epidermis eventually fuses to form a stolonal mat. Upon reaching sexual maturity the colony, which now consists of hundreds of polyps, will bud a new polyp type, the sexual polyp, which will give rise to the gametes.

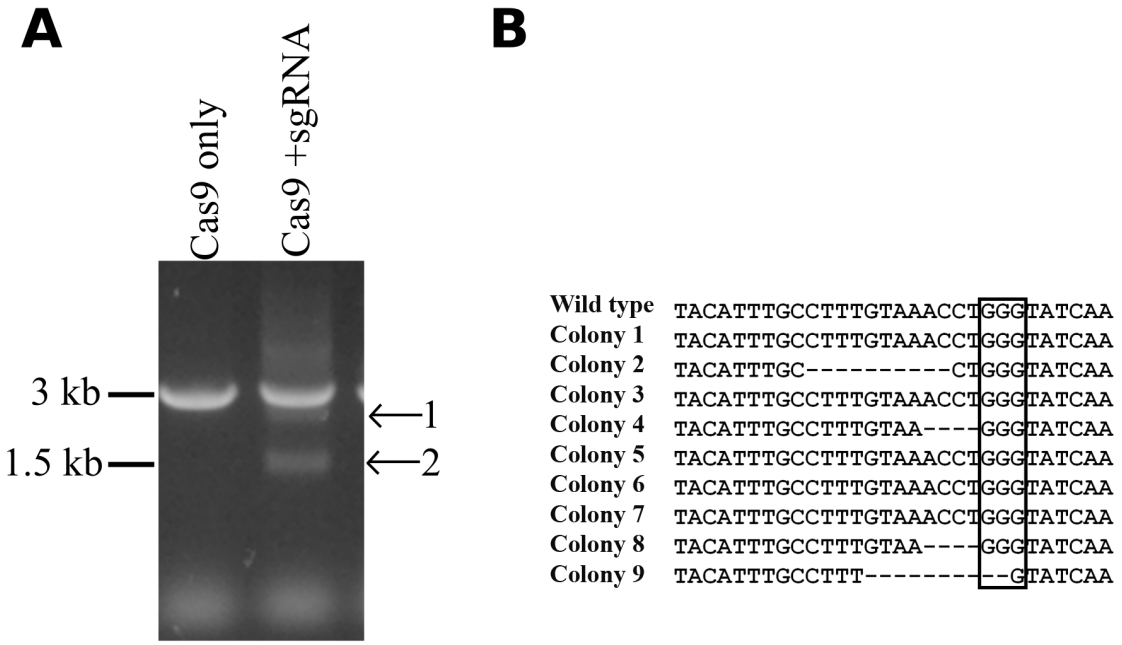

C

	Wild type alleles	One or more mutations
Experiment 1	3/9	6/9 (66.6%)
Experiment 2	2/7	5/7 (71.4%)

Figure S2. Development of a CRIPSR-Cas9 protocol to study *Notch* function in *Hydractinia* (**A**) Agarose gel showing the PCR product across the targeted exons in control and injected larva. Note the lower bands in the Cas9 + sgRNA lane. (**B**) Example of the mutations found at one sgRNA cutting site in sequenced clones from the upper band from an individual experiment. (**C**) The number of mutated alleles at one or more sgRNA site in two independent biological replicates.

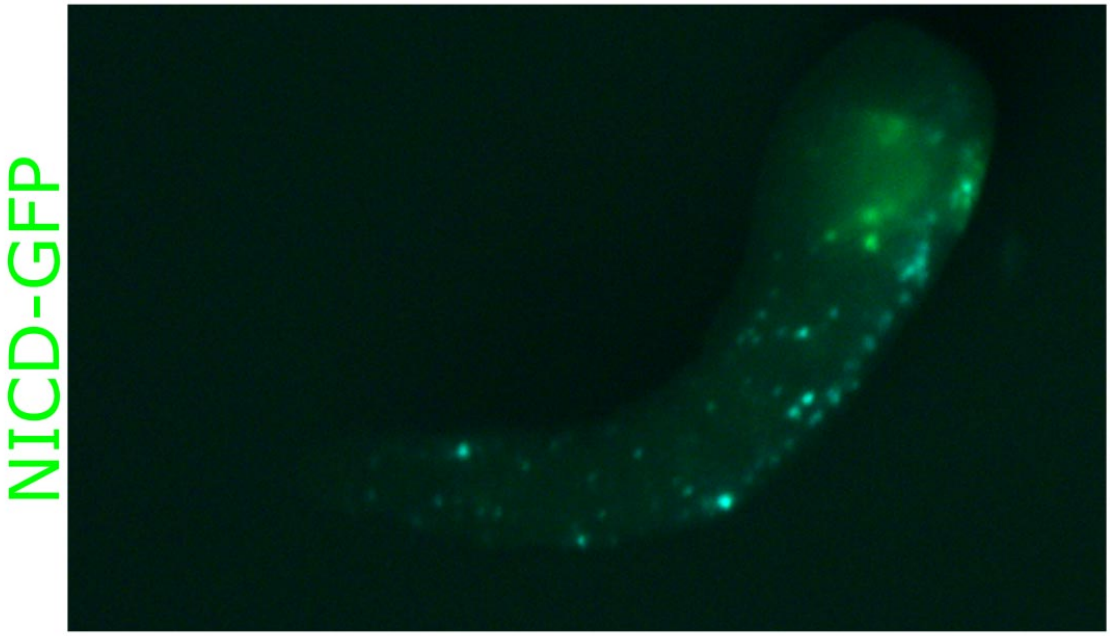

Figure S3. Transgenic mosaic larva expressing NICD-GFP.

SUPPLEMENTAL REFERENCES

Bolger, A. M., Lohse, M. and Usadel, B. (2014). Trimmomatic: a flexible trimmer for Illumina sequence data. *Bioinformatics* **30**.

Chirgwin, J. M., Przybyla, A. E., MacDonald, R. J. and Rutter, W. J. (1979). Isolation of biologically active ribonucleic acid from sources enriched in ribonuclease. *Biochemistry* **18**.

Gazave, E., Lapebie, P., Richards, G. S., Brunet, F., Ereskovsky, A. V., Degnan, B. M., Borchiellini, C., Vervoort, M. and Renard, E. (2009). Origin and evolution of the Notch signalling pathway: an overview from eukaryotic genomes. *BMC evolutionary biology* **9**, 249.

Haas, B. J., Papanicolaou, A., Yassour, M., Grabherr, M., Blood, P. D. and Bowden, J. (2013). De novo transcript sequence reconstruction from RNA-seq using the Trinity platform for reference generation and analysis. Nat Protoc. Nature Publishing. *Group* **8**.

Kanska, J. and Frank, U. (2013). New roles for Nanos in neural cell fate determination revealed by studies in a cnidarian. *J Cell Sci* **126**, 3192-3203.

Kim, D., Pertea, G., Trapnell, C., Pimentel, H., Kelley, R. and Salzberg, S. L. (2013). TopHat2: accurate alignment of transcriptomes in the presence of insertions, deletions and gene fusions. *Genome Biology* **14**, R36.

Li, B. and Dewey, C. N. (2011). RSEM: accurate transcript quantification from RNA-Seq data with or without a reference genome. *BMC Bioinformatics* **12**, 323.

Pertea, M., Pertea, G. M., Antonescu, C. M., Chang, T. C., Mendell, J. T. and Salzberg, S. L. (2015). StringTie enables improved reconstruction of a transcriptome from RNA-seq reads. *Nature biotechnology* **33**, 290-295.

Robinson, M. D., McCarthy, D. J. and Smyth, G. K. (2010). edgeR: a Bioconductor package for differential expression analysis of digital gene expression data. *Bioinformatics* **26**.

Török, A., Schiffer, P. H., Schnitzler, C. E., Ford, K., Mullikin, J. C., Baxevanis, A. D., Bacic, A., Frank, U. and Gornik, S. G. (2016). The cnidarian Hydractinia echinata employs canonical and highly adapted histones to pack its DNA. *Epigenetics & Chromatin* **9**, 1-17.

Trapnell, C., Roberts, A., Goff, L., Pertea, G., Kim, D., Kelley, D. R., Pimentel, H., Salzberg, S. L., Rinn, J. L. and Pachter, L. (2012). Differential gene and transcript expression analysis of RNA-seq experiments with TopHat and Cufflinks. *Nature protocols* **7**, 562-578.

Wolenski FS, Layden MJ, Martindale MQ, Gilmore TD, Finnerty JR. (2013). Characterizing the spatiotemporal expression of RNAs and proteins in the starlet sea anemone, Nematostella vectensis. *Nature Protocols*. 8: 900-915.